J. Fluid Mech. (1978), *vol.* 86, *part* 4, *pp.* 727–744
Printed in Great Britain

Stokes flow due to a Stokeslet in a pipe

By N. LIRON AND R. SHAHAR
Department of Applied Mathematics, The Weizmann Institute of Science, Rehovot, Israel

(Received 19 September 1977)

Velocity and pressure fields for Stokes flow due to a force singularity (Stokeslet) of arbitrary orientation and at arbitrary location inside an infinite circular pipe are obtained. Two alternative expressions for the solution, one in terms of a Fourier–Bessel type expansion, and the other as a doubly infinite series, are given. The latter is especially suitable for computational purposes as it is shown to be an exponentially decaying series. From the series it is found that all velocity components decay exponentially to zero up- or downstream away from the Stokeslet. This is also true for pressure fields of Stokeslets perpendicular to the axis of the pipe. A Stokeslet parallel to the axis of the pipe raises the pressure difference between $-\infty$ to $+\infty$ by a finite non-zero amount. Some numerical results for a Stokeslet parallel to the axis are given. Comparison of the results with flow in a two-dimensional channel is also discussed.

1. Introduction

In a wide range of animal and plant structures the outer cells of a surface have hair-like active extensions called cilia. These cilia move in an organized fashion to produce flow in the fluid bathing them.

A great deal of attention has been given in recent years to fluid movement due to cilia in order to try and understand how cilia perform their function, whether it is the propulsion of micro-organisms or the transport of fluid and particles through pipes the walls of which are covered by cilia. A detailed description and a discussion of ciliary motion can be found in Blake & Sleigh (1974), together with an extensive bibliography. For propulsion of micro-organisms Blake & Sleigh describe two models used to portray the motion of cilia. The first is the envelope approach found to be valid for symplectic metachronism. For antiplectic metachronism the envelope approach is not satisfactory, and this led to the second model, the 'cilia sublayer model' or 'discrete-cilia model', initiated by Blake (1972) and further developed and extended by Liron & Mochon (1976*a*).

In the discrete model one approximates each cilium by a line of force singularities (Stokeslets) along the centre-line. The velocity field due to all cilia is then found by summing over all cilia. Thus, the basic solution needed is the solution to Stokes flow due to Stokeslets in the appropriate region. The solution for a Stokeslet above a flat plate was given by Blake (1971), and previously by Lorentz (1896).

Lardner & Shack (1972) used the envelope model to calculate the rate of flow of sperm through the ductus efferentes of the male reproductive tract, and obtained results about 50 times smaller than observed rates. This is an indication that the envelope model is inappropriate and the discrete-cilia approach has to be used. Liron (1978)

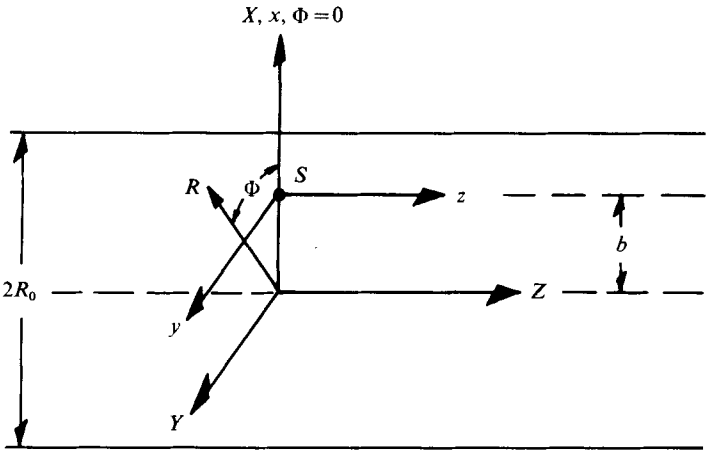

FIGURE 1. Geometric configuration of the problem and the three co-ordinate systems used. X, Y, Z and x, y, z Cartesian co-ordinates. R, Φ, Z cylindrical co-ordinates. The Stokeslet is at S.

used the solution for a Stokeslet between two parallel plates given by Liron & Mochon (1976*b*), to deal with fluid transport between two plates, as an approximation for fluid transport in a pipe. The justification for using the parallel-plates, or channel, model lies in the similarity, if it exists, between flow in a pipe and in a channel. In order to justify this approximation, and also to develop a suitable pipe model, the Stokes flow solution due to a Stokeslet in a pipe, at arbitrary location and arbitrary orientation, is needed. This solution is presented in this paper.

The problem is formulated in § 2. In § 3 the singular infinite solution is transformed into a Fourier–Bessel type expansion. The auxiliary solution needed in order to satisfy the no-slip boundary conditions on the pipe wall is given in § 4, again as a Fourier–Bessel expansion. This solution is transformed into a doubly infinite series, amenable to computational purposes, in § 5, using contour integration. The zeroes of the denominators used in § 5 are given and discussed in § 6, and it is shown that all doubly infinite series decay exponentially with distance along the axis of the pipe. The above series are used in § 7 to compute velocities and pressures, and various results are depicted. These results, and some common features with flow between parallel plates, are discussed in § 8.

2. Formulation of the problem

Consider a force singularity (Stokeslet) in a viscous incompressible fluid inside a straight circular infinite pipe of radius R_0. We shall look at three co-ordinate systems. The first system is a cylindrical co-ordinate system R, Φ, Z, and is chosen such that the Stokeslet is situated at $b, 0, 0$, see figure 1.

The second system is a Cartesian co-ordinate system X, Y, Z, with origin at the origin of the cylindrical system and the same Z axis. The X axis passes through the Stokeslet, and the Y axis completes the two. In this co-ordinate system the Stokeslet is at $b, 0, 0$. The third system is also a Cartesian co-ordinate system x, y, z, parallel to the previous system, but shifted so that the Stokeslet in this system is at $0, 0, 0$.

We are looking for the fundamental singular solutions (velocities and pressure) of the

Stokeslet situated as described above, and satisfying the no-slip boundary conditions on the pipe wall $R = R_0$.

There are three different sets of solutions corresponding to three independent directions of the Stokeslet, and we choose the directions x, y, z, which also correspond to the directions R, Φ, Z at the Stokeslet. In the x, y, z system we shall denote the three sets of solutions for the pressure and velocity, respectively, by

$$P^k, \mathbf{u}^k = (u_j^k), \quad j = 1, 2, 3, \quad k = 1, 2, 3, \tag{2.1}$$

where $k = 1, 2, 3$ corresponds to a Stokeslet pointing in the x, y, z directions, respectively, and $j = 1, 2, 3$ corresponds to the components of velocity in the x, y, z directions, respectively. Alternatively, if we want the velocities in the R, Z, Φ directions, we shall use the explicit notation u_R^k, u_Φ^k, u_z^k.

The functions P^k and $\mathbf{u}^k$ are the solutions of the Stokes equations

$$\nabla P^k = \mu \nabla^2 \mathbf{u}^k + \delta(r)\, \mathbf{e}^k, \tag{2.2}$$

$$\nabla . \mathbf{u}^k = 0, \tag{2.3}$$

with the boundary conditions

$$\mathbf{u}^k = 0 \quad \text{at} \quad R = R_0, \tag{2.4}$$

$$\mathbf{u}^k \to 0, \quad Z \to \pm \infty. \tag{2.5}$$

Here $\mathbf{e}^k$ is a unit vector in the k direction, as above, μ is the viscosity, and

$$r = (x^2 + y^2 + z^2)^{\frac{1}{2}}. \tag{2.6}$$

The solution to (2.2) and (2.3) in an infinite fluid (i.e. the solution decaying to zero at $r \to \infty$) is given by (see, e.g., Blake 1971)

$$v_j^k = \frac{1}{8\pi\mu}\left[\frac{\delta_{jk}}{r} + \frac{x_j x_k}{r^3}\right], \tag{2.7}$$

$$P_1^k = \frac{1}{4\pi}\frac{x_k}{r^3}, \tag{2.8}$$

where we have used the notation $x, y, z \equiv x_1, x_2, x_3$. This solution takes care of the singularity in (2.2) and we are left to solve for the correction, i.e. to solve for

$$\nabla p^k = \mu \nabla^2 \mathbf{g}^k, \tag{2.9}$$

$$\nabla . \mathbf{g}^k = 0, \tag{2.10}$$

with the boundary conditions

$$\mathbf{g}^k(R = R_0) = -\mathbf{v}^k(R = R_0), \tag{2.11}$$

$$\mathbf{g}^k \to 0, \quad Z \to \pm \infty. \tag{2.12}$$

The complete solution is then

$$\mathbf{u}^k = \mathbf{v}^k + \mathbf{g}^k, \quad P^k = P_1^k + p^k. \tag{2.13}$$

3. Transformation of singular solution

The general solution to (2.9) and (2.10), with arbitrary prescribed boundary conditions on the surface of the pipe, is given by Happel & Brenner (1973) in the form of a Fourier–Bessel type expansion, see §4 below. In order to use this solution it is necessary to express v_j^k, P_1^k given in (2.7), (2.8) in the same form.

Happel & Brenner (1973, p. 304) give the following relations:

$$\frac{1}{r} = \begin{cases} \frac{2}{\pi}\sum_{k=-\infty}^{\infty} \cos k\Phi \int_0^\infty K_k(\lambda b)\, I_k(\lambda R)\cos\lambda z\, d\lambda, & R < b, \\ \frac{2}{\pi}\sum_{k=-\infty}^{\infty} \cos k\Phi \int_0^\infty I_k(\lambda b)\, K_k(\lambda R)\cos\lambda z\, d\lambda, & b < R, \end{cases} \tag{3.1}$$

and

$$\frac{z}{r} = \begin{cases} -\frac{2}{\pi}\sum_{k=-\infty}^{\infty} \cos k\Phi \int_0^\infty [RK_k'(\lambda R)\, I_k(\lambda b) + bK_k(\lambda R)\, I_k'(\lambda b)]\sin\lambda z\, d\lambda, & R > b, \\ -\frac{2}{\pi}\sum_{k=-\infty}^{\infty} \cos k\Phi \int_0^\infty [RI_k'(\lambda R)\, K_k(\lambda b) + bI_k(\lambda R)\, K_k'(\lambda b)]\sin\lambda z\, d\lambda, & R < b, \end{cases} \tag{3.2}$$

where a prime denotes differentiation with respect to the argument.

Using relations such as

$$\frac{xz}{r^3} = -\frac{\partial}{\partial x}\left(\frac{z}{r}\right); \quad \frac{yz}{r^3} = -\frac{\partial}{\partial y}\left(\frac{z}{r}\right); \quad \frac{1}{r} + \frac{z^2}{r^3} = \frac{2}{r} - \frac{\partial}{\partial z}\left(\frac{z}{r}\right), \tag{3.3}$$

and the relations between the co-ordinate systems,

$$X^2 + Y^2 = R^2, \quad X = R\cos\Phi, \quad Y = R\sin\Phi, \quad x = X - b, \tag{3.4}$$

which lead to the relations

$$\frac{\partial}{\partial x} = \cos\Phi\frac{\partial}{\partial R} - \frac{\sin\Phi}{R}\frac{\partial}{\partial\Phi}; \quad \frac{\partial}{\partial y} = \sin\Phi\frac{\partial}{\partial R} + \frac{\cos\Phi}{R}\frac{\partial}{\partial\Phi}, \tag{3.5}$$

we obtain (after some tedious algebra) the following expressions for the velocities:

$$\left.\begin{aligned} 4\pi^2\mu v_j^j &= \sum_{k=-\infty}^{\infty} \cos k\Phi \int_0^\infty f_j^j(\lambda, R, k, b)\cos\lambda z\, d\lambda, \quad j = 1, 2, 3, \\ 4\pi^2\mu v_2^1 &= 4\pi^2\mu v_1^2 = \sum_{k=-\infty}^{\infty} \sin k\Phi \int_0^\infty f_2^1(\lambda, R, k, b)\cos\lambda z\, d\lambda, \\ 4\pi^2\mu v_3^1 &= 4\pi^2\mu v_1^3 = \sum_{k=-\infty}^{\infty} \cos k\Phi \int_0^\infty f_3^1(\lambda, R, k, b)\sin\lambda z\, d\lambda, \\ 4\pi^2\mu v_3^2 &= 4\pi^2\mu v_2^3 = \sum_{k=-\infty}^{\infty} \sin k\Phi \int_0^\infty f_3^2(\lambda, R, k, b)\sin\lambda z\, d\lambda, \end{aligned}\right\} \tag{3.6}$$

and for the pressure

$$\left.\begin{aligned} 2\pi^2 P_1^1 &= \sum_{k=-\infty}^{\infty} \cos k\Phi \int_0^\infty t^1(\lambda, R, k, b) \cos \lambda z \, d\lambda, \\ 2\pi^2 P_1^2 &= \sum_{k=-\infty}^{\infty} \sin k\Phi \int_0^\infty t^2(\lambda, R, k, b) \cos \lambda z \, d\lambda, \\ 2\pi^2 P_1^3 &= \sum_{k=-\infty}^{\infty} \cos k\Phi \int_0^\infty t^3(\lambda, R, k, b) \sin \lambda z \, d\lambda, \end{aligned}\right\} \tag{3.7}$$

where the functions f_j^k, t^k are given in appendix A. Once these functions are known we can proceed to find the auxiliary solutions g_j^k, p^k.

4. The auxiliary solution

The general solution to (2.9) and (2.10) is given by Happel & Brenner (1973, p. 77) as

$$\mathbf{g} = \nabla\psi + \nabla \times (\Omega \mathbf{e}^3) + R \frac{\partial}{\partial R}(\nabla\pi) + \mathbf{e}^3 \frac{\partial \pi}{\partial z}, \tag{4.1}$$

$$p = -2\mu \frac{\partial^2 \pi}{\partial z^2}. \tag{4.2}$$

Here π, ψ, Ω are harmonic functions and are given by

$$\left.\begin{aligned} \pi &= \sum_{k=-\infty}^{\infty} \cos(k\Phi + \alpha_k^1) \int_0^\infty \pi_k(\lambda) I_k(\lambda R) \cos(\lambda z + \delta_\lambda^1) \, d\lambda, \\ \psi &= \sum_{k=-\infty}^{\infty} \cos(k\Phi + \alpha_k^2) \int_0^\infty \psi_k(\lambda) I_k(\lambda R) \cos(\lambda z + \delta_\lambda^2) \, d\lambda, \\ \Omega &= \sum_{k=-\infty}^{\infty} \cos(k\Phi + \alpha_k^3) \int_0^\infty \omega_k(\lambda) I_k(\lambda R) \cos(\lambda z + \delta_\lambda^3) \, d\lambda, \end{aligned}\right\} \tag{4.3}$$

where $\pi_k(\lambda)$, $\psi_k(\lambda)$, $\omega_k(\lambda)$ and the phases α_k^j, δ_λ^j are to be determined by the prescribed boundary conditions. Writing (4.1) explicitly, and substituting for π, ψ, Ω from (4.3), we obtain, for the three components of velocity in the R, Φ, Z directions, the expressions

$$\begin{aligned} g_R = \sum_{k=-\infty}^{\infty} \int_0^\infty \{ & \cos(k\Phi + \alpha_k^2) \psi_k(\lambda) \lambda I_k'(\lambda R) \cos(\lambda z + \delta_\lambda^2) \\ & - \sin(k\Phi + \alpha_k^3) \omega_k(\lambda) (k/R) I_k(\lambda R) \cos(\lambda z + \delta_\lambda^3) \\ & + \cos(k\Phi + \alpha_k^1) \lambda^2 R \pi_k(\lambda) I_k''(\lambda R) \cos(\lambda z + \delta_\lambda^1) \} \, d\lambda, \end{aligned} \tag{4.4}$$

$$\begin{aligned} g_\Phi = \sum_{k=-\infty}^{\infty} \int_0^\infty \{ & -\sin(k\Phi + \alpha_k^2) (k/R) \psi_k(\lambda) I_k(\lambda R) \cos(\lambda z + \delta_\lambda^2) \\ & - \cos(k\Phi + \alpha_k^3) \omega_k(\lambda) \lambda I_k'(\lambda R) \cos(\lambda z + \delta_\lambda^3) \\ & + \sin(k\Phi + \alpha_k^1) (k/R) \pi_k(\lambda) I_k(\lambda R) \cos(\lambda z + \delta_\lambda^1) \\ & - \sin(k\Phi + \alpha_k^1) k \pi_k(\lambda) \lambda I_k'(\lambda R) \cos(\lambda z + \delta_\lambda^1) \} \, d\lambda, \end{aligned} \tag{4.5}$$

$$\begin{aligned} g_z = \sum_{k=-\infty}^{\infty} \int_0^\infty \{ & -\cos(k\Phi + \alpha_k^2) \lambda \psi_k(\lambda) I_k(\lambda R) \sin(\lambda z + \delta_\lambda^2) \\ & - \cos(k\Phi + \alpha_k^1) [\lambda^2 R I_k'(\lambda R) + \lambda I_k(\lambda R)] \pi_k(\lambda) \sin(\lambda z + \delta_\lambda^1) \} \, d\lambda. \end{aligned} \tag{4.6}$$

For the pressure we obtain

$$p = 2\mu \sum_{k=-\infty}^{\infty} \int_0^{\infty} \cos(k\Phi + \alpha_k^1)\, \lambda^2 \pi_k(\lambda)\, I_k(\lambda R) \cos(\lambda z + \delta_\lambda^1)\, d\lambda. \tag{4.7}$$

In order to satisfy the boundary conditions (2.11) we have to match corresponding velocities. In §3 velocities are given in the x, y, z directions, and above in the R, Φ, Z directions. We can transform either of them to the other form. We choose to transform g_R, g_Φ, g_z into g_x, g_y, g_z. This is achieved through

$$\begin{aligned} g_x &= g_R \cos\Phi - g_\Phi \sin\Phi, \\ g_y &= g_R \sin\Phi + g_\Phi \cos\Phi, \quad g_z = g_z. \end{aligned} \tag{4.8}$$

After transforming and rearranging one can now satisfy the boundary conditions (2.11) term by term in the Fourier sum. We have to deal with each of the three directions of the Stokeslet separately.

(a) *Stokeslet in x direction.* In this case we choose

$$\alpha_k^1 = \alpha_k^2 = \delta_\lambda^1 = \delta_\lambda^2 = \delta_\lambda^3 = 0, \quad \alpha_k^3 = -\tfrac{1}{2}\pi, \tag{4.9}$$

in (4.4)–(4.7). Using (4.8), rearranging and equating the Fourier coefficients term by term in (2.11), we obtain the following system of equations:

$$\begin{bmatrix} \lambda I_{k+1}(s) & -\lambda I_{k+1}(s) & \lambda s I'_{k+1}(s) \\ \lambda I_{k-1}(s) & \lambda I_{k-1}(s) & \lambda s I'_{k-1}(s) \\ -\lambda I_k(s) & 0 & -[\lambda s I'_k(s) + \lambda I_k(s)] \end{bmatrix} \begin{bmatrix} \psi_k^1(\lambda) \\ \omega_k^1(\lambda) \\ \pi_k^1(\lambda) \end{bmatrix} = \begin{bmatrix} H_k^1 \\ G_k^1 \\ L_k^1 \end{bmatrix}, \tag{4.10}$$

where

$$s \equiv \lambda R_0, \tag{4.11}$$

and the functions H^1, G^1 and L^1 are

$$\left.\begin{aligned} H_k^1 &= -\frac{1}{4\pi^2\mu}[f_1^1(\lambda, R_0, k+1, b) + f_2^1(\lambda, R_0, k+1, b)], \\ G_k^1 &= -\frac{1}{4\pi^2\mu}[f_1^1(\lambda, R_0, k-1, b) - f_2^1(\lambda, R_0, k-1, b)], \\ L_k^1 &= -\frac{1}{4\pi^2\mu} f_3^1(\lambda, R_0, k, b), \end{aligned}\right\} \tag{4.12}$$

and f_j^i are given in appendix A.

The solution to (4.10)–(4.12) is

$$\left.\begin{aligned} \Delta_k(\lambda)\,\psi_k^1(\lambda) &= -s[I_{k-1}(s)\, I_{k+1}(s)]'\, L_k^1 - (sI_k(s))'\,[I_{k-1}(s)\, H_k^1 + I_{k+1}(s)\, G_k^1], \\ \Delta_k(\lambda)\,\omega_k^1(\lambda) &= [sI_k(s)\, I'_{k+1}(s) - I_{k+1}(s)\,(sI_k(s))']\, G_k^1 \\ &\quad + [(sI_k(s))'\, I_{k-1}(s) - sI_k(s)\, I'_{k-1}(s)]\, H_k^1 + [I_{k-1}(s)\, I'_{k+1}(s) \\ &\quad - I'_{k-1}(s)\, I_{k+1}(s)]\, sL_k^1, \\ \Delta_k(\lambda)\,\pi_k^1(\lambda) &= I_k(s)\,[G_k^1 I_{k+1}(s) + H_k^1 I_{k-1}(s)] + 2L_k^1 I_{k-1}(s)\, I_{k+1}(s), \end{aligned}\right\} \tag{4.13}$$

where

$$\Delta_k(\lambda) = \lambda[sI_k(s)\,(I_{k-1}(s)\, I_{k+1}(s))' - 2(sI_k(s))'\, I_{k-1}(s)\, I_{k+1}(s)]. \tag{4.14}$$

This completes the solution in this case.

(*b*) *Stokeslet in y direction.* In this case we choose

$$\delta_\lambda^1 = \delta_\lambda^2 = \delta_\lambda^3 = \alpha_k^3 = 0, \quad \alpha_k^1 = \alpha_k^2 = -\tfrac{1}{2}\pi, \tag{4.15}$$

in (4.4)–(4.7). Repeating the same procedure as before we now get for $\psi_k^2(\lambda)$, $\omega_k^2(\lambda)$ and $\pi_k^2(\lambda)$ the same expressions as in (4.13), with the following changes: H_k^1, G_k^1 and L_k^1 are replaced by H_k^2, G_k^2, L_k^2 which are

$$\left.\begin{aligned} H_k^2 &= -\frac{1}{4\pi^2\mu}[f_1^2(\lambda R_0, k+1, b) - f_2^2(\lambda, R_0, k+1, b)], \\ G_k^2 &= -\frac{1}{4\pi^2\mu}[f_1^2(\lambda, R_0, k-1, b) + f_2^2(\lambda, R_0, k-1, b)], \\ L_k^2 &= -\frac{1}{4\pi^2\mu} f_3^2(\lambda, R_0, k, b), \end{aligned}\right\} \tag{4.16}$$

and for $\Delta_k(\lambda)\,\omega_k^2(\lambda)$ we have to change the sign of the entire right-hand side in (4.13).

(*c*) *Stokeslet in z direction.* In this case we choose

$$\alpha_k^1 = \alpha_k^2 = 0, \quad \alpha_k^3 = \delta_\lambda^1 = \delta_\lambda^2 = \delta_\lambda^3 = -\tfrac{1}{2}\pi, \tag{4.17}$$

in (4.4)–(4.7). Again, we now get for $\psi_k^3(\lambda)$, $\omega_k^3(\lambda)$, $\pi_k^3(\lambda)$ the same expressions as in (4.13) with the following changes: H_k^1, G_k^1 and L_k^1 are replaced by H_k^3, G_k^3 and L_k^3 which are

$$\left.\begin{aligned} H_k^3 &= -\frac{1}{4\pi^2\mu}[f_1^3(\lambda, R_0, k+1, b) + f_2^3(\lambda, R_0, k+1, b)], \\ G_k^3 &= -\frac{1}{4\pi^2\mu}[f_1^3(\lambda, R_0, k-1, b) - f_2^3(\lambda, R_0, k-1, b)], \\ L_k^3 &= \frac{1}{4\pi^2\mu} f_3^3(\lambda, R_0, k, b). \end{aligned}\right\} \tag{4.18}$$

This completes the solution for all three cases, but it is obvious that very little information can be obtained from the solution in this form. In order to obtain more insight into the solutions, and to be able to compute velocities and pressures, we shall transform this solution to a form amenable for computational purposes. This will be done in the next section.

5. Alternative form of the solution

As can be seen from (4.4)–(4.7), (4.12)–(4.14), (4.16), (4.18) and appendix A, if we divide numerator and denominator [which is $\Delta_k(\lambda)$ given in (4.14)] by λ, we can express all integrals in terms of the variables λR_0, λR, λb, and λz. Changing then to integration over $s = \lambda R_0$, and non-dimensionalizing R, b, z by R_0, velocities by $1/\mu R_0$ and pressure by $1/R_0^2$ (the last two are multiplied by force to get the proper dimensions), we can express ψ_k, ω_k and π_k and the integrals as functions of $s = \lambda R_0$, sz, sb and sR, where z, b, and R are now non-dimensionalized.

The denominator in ψ_k, π_k, ω_k is now

$$D_k(s) = sI_k(s)\,(I_{k-1}(s)\,I_{k+1}(s))' - 2(sI_k(s))'\,I_{k-1}(s)\,I_{k+1}(s). \tag{5.1}$$

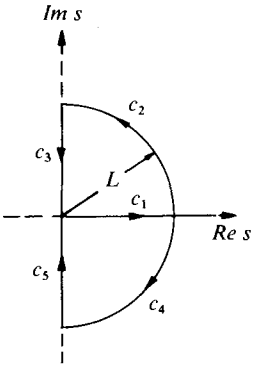

FIGURE 2. The contours of integration in the complex s plane.

The general form of the solution for the velocities and pressure is

$$u_j^k = \sum_{k=-\infty}^{\infty} \frac{\sin k\Phi}{\cos k\Phi} \int_0^\infty \left[f_j^k(s,k,R,b) + \frac{F_j^k(s,k,R,b)}{D_k(s)} \right] \frac{\sin sz}{\cos sz} ds. \tag{5.2}$$

In what follows we shall assume $z > 0$. If $z < 0$ then $u_j^k(z) = \pm u_j^k(-z)$ depending on whether we have $\cos sz$ or $\sin sz$ in the integral.

Consider the following two integrals in the complex s plane, see figure 2, for $L \to \infty$:

$$\int_{c_1c_2c_3} \tfrac{1}{2}[f_j^k + F_j^k/D_k] \exp(isz)\, ds; \tag{5.3}$$

$$\int_{c_1c_4c_5} \tfrac{1}{2}[f_j^k + F_j^k/D_k] \exp(-isz)\, ds. \tag{5.4}$$

For $\cos sz$ we take the sum of the two, and for $\sin sz$ the difference of the two (divided by i).

It can be shown that in all cases the following hold:

$$\lim_{L\to\infty} \int_{c_3} = \lim_{L\to\infty} \int_{c_4} = 0, \tag{5.5}$$

$$\lim_{L\to\infty} \left[\int_{c_3} + \int_{c_5} \right] = 0, \tag{5.6}$$

for the $\cos sz$ cases, and

$$\lim_{L\to\infty} \left[\int_{c_3} - \int_{c_5} \right] = 0, \tag{5.7}$$

for the $\sin sz$ cases. The proof of (5.5)–(5.7) for all cases is straightforward but tedious and will not be reproduced here.

We are therefore left with the integrals in (5.2) being equal to the sum of residues due to $D_k(s)$, in the first and fourth quadrants.

As will be seen in the next section there are three types of roots for $D_k(s)$ in the first quadrant:

(1) a sequence of complex roots which we denote by

$$x_n = a_n + ib_n, \quad n = 1, 2, \ldots, \tag{5.8}$$

(2) a sequence of imaginary roots which we denote by

$$y_n = ic_n, \quad n = 0, 1, 2, \ldots, \tag{5.9}$$

(3) a root at the origin, $s = 0$.

The roots in the fourth quadrant are the complex conjugates of those in the first quadrant.

It follows that residues from x_n will be multiplied by $2\pi i$, residues from y_n by πi, and residues from the origin by $\frac{1}{2}\pi i$ (excluding the origin in the contour integration). It turns out that there are no residues from the origin for all velocities. For the pressure the only possible residue from the origin is for the $k = 0$ term in (4.7). In the cases (*a*) and (*b*) in § 4, (4.7) will have $\cos \lambda z$ under the integral sign. The residue from the origin, if any, will therefore add a constant, and pressure is defined anyway up to an additive constant. In case (*c*), of a Stokeslet in the z direction, (4.7) has $\sin \lambda z$ under the integral sign. It follows that the residue at the origin will add a constant for $z > 0$, and its negative for $z < 0$, and so must be considered.

The full expressions for the velocities and pressure, using the above procedure, are given in appendix B.

6. The roots of $D_k(s)$ and the far field

For the computation of the residues as described in the previous section, we need the roots of $D_k(s)$ given in (5.1), in the first quadrant. If s is a root, so are $-s$, $\pm\bar{s}$, so we shall look at the roots in the first quadrant of

$$\tilde{D}_k(s) = s[J_k^2(s) - J_{k-1}(s)\,J_{k+1}(s)]\,[J_{k-1}(s) - J_{k+1}(s)] - 4J_{k-1}(s)\,J_k(s)\,J_{k+1}(s). \tag{6.1}$$

If $s = b + ia$ is a root in the first quadrant of $\tilde{D}_k(s)$ then $i\bar{s} = a + ib$ is a root of $D_k(s)$ in the first quadrant.

Clearly $\tilde{D}_k(s)$ has a root at $s = 0$.

To get an estimate for the other roots let us look at the asymptotic formula for $J_k(s)$. From Abramowitz & Stegun (1965)

$$J_k(s) \sim (2/\pi s)^{\frac{1}{2}} \cos(s - \tfrac{1}{4}\pi - \tfrac{1}{2}k\pi), \quad s > \tfrac{1}{2}k\pi. \tag{6.2}$$

If $y = s - \frac{1}{4}\pi - \frac{1}{2}k\pi$, then substituting (6.2) into (6.1) we get

$$(s - \sin 2y)\sin y \sim 0. \tag{6.3}$$

from which we get two possible sequences:

(i) $\sin y \sim 0$, from which we obtain for the roots of $D_k(s)$,

$$y_n = ic_n \sim i[\tfrac{1}{4}\pi + \tfrac{1}{2}k\pi + n\pi], \quad n = 0, 1, \ldots; \tag{6.4}$$

(ii) $s \sim \sin 2y$, from which we obtain for the roots of $D_k(s)$,

$$x_n = a_n + ib_n \sim \tfrac{1}{2}\ln[(2n + k + 1)\pi] + (2n + k + 1)\tfrac{1}{2}\pi i, \quad n = 0, 1, \ldots. \tag{6.5}$$

Equation (6.4) gives the asymptotic estimates for the imaginary roots, and (6.5) those for the complex roots. In table 1 we give the first four imaginary roots for each k, for $k = 0, \ldots, 10$. The roots of $k = 0$ are the roots of $I_1(s)$, see also appendix B. In table 2 we give the first three complex roots for each k, for $k = 0, \ldots, 10$.

If we look at the detailed expressions for the velocities and pressure given in appendix B, we see that for each k in the outer sum we have two inner sums. Both are

	n			
k	1	2	3	4
0	3·8317i	7·0156i	10·173i	13·324i
1	5·3172i	8·5330i	11·705i	14·863i
2	6·6741i	9·9607i	13·167i	16·346i
3	7·9678i	11·332i	14·580i	17·785i
4	9·2218i	12·663i	15·955i	19·191i
5	10·448i	13·963i	17·301i	20·569i
6	11·653i	15·240i	18·624i	21·924i
7	12·841i	16·497i	19·926i	23·259i
8	14·016i	17·738i	21·211i	24·576i
9	15·180i	18·965i	22·481i	25·879i
10	16·334i	20·181i	23·739i	27·169i

TABLE 1. The first four imaginary roots $y_n(k)$ of $D_k(s)$, see (5.1), (5.9), in the first quadrant, for $k = 0, \ldots, 10$.

	n		
k	1	2	3
0	—	1·4675 + 4·4663i	1·7270 + 7·6941i
1	1·1226 + 2·5678i	1·6081 + 6·0038i	1·8169 + 9·2322i
2	1·3119 + 3·9145i	1·7140 + 7·4157i	1·8926 + 10·684i
3	1·4476 + 5·1597i	1·8024 + 8·7586i	1·9594 + 12·080i
4	1·5576 + 6·3562i	1·8796 + 10·056i	2·0197 + 12·434i
5	1·6518 + 7·5229i	1·9489 + 11·322i	2·0750 + 14·757i
6	1·7349 + 8·6692i	2·0122 + 12·563i	2·1264 + 16·055i
7	1·8100 + 9·8004i	2·0706 + 13·785i	2·1745 + 17·332i
8	1·8786 + 10·920i	2·1251 + 14·991i	2·2199 + 18·592i
9	1·9421 + 12·030i	2·1763 + 16·184i	2·2629 + 19·837i
10	2·0013 + 12·132i	2·2247 + 17·365i	2·3038 + 21·069i

TABLE 2. The first three complex roots $x_n(k)$ of $D_k(s)$, see (5.1), (5.8), in the first quadrant, for $k = 0, 1, \ldots, 10$.

exponentially decreasing series, with the first decaying like $\exp(-b_0 z)$ and the second like $\exp(-c_0 z)$. For the behaviour of b_0 and c_0 with k we look at tables 1 and 2. From table 1 we see that $c_0(k) > c_0(1) + k$, and from table 2 that $b_0(k) > b_0(0) + k$. Thus summing over the outer series, we get that the total expressions decay exponentially with z, at least as fast as $\exp(-2{\cdot}57z)$. The functions F^j and l^j in (B 3) cause no problem as they behave like $\exp(-s(1-R_0))\exp(-s(1-b))$ for $|s| \gg 1$. We thus get that all velocity components decay exponentially with z, and so do P^1 and P^2. P^3 tends exponentially to its value at $z = \infty$, which is $(1-b^2)/\pi$, from (B 3). In the dimensional variables we get therefore that a Stokeslet pointing in the z direction will raise the pressure from

$$P^3 \to -\frac{1}{\pi R_0^2}\left(1-\left(\frac{b}{R_0}\right)^2\right), \quad z \to -\infty, \tag{6.6}$$

to

$$P^3 \to +\frac{1}{\pi R_0^2}\left(1-\left(\frac{b}{R_0}\right)^2\right), \quad z \to +\infty, \tag{6.7}$$

and the approach to these limiting values is exponential with $|z| \to \infty$.

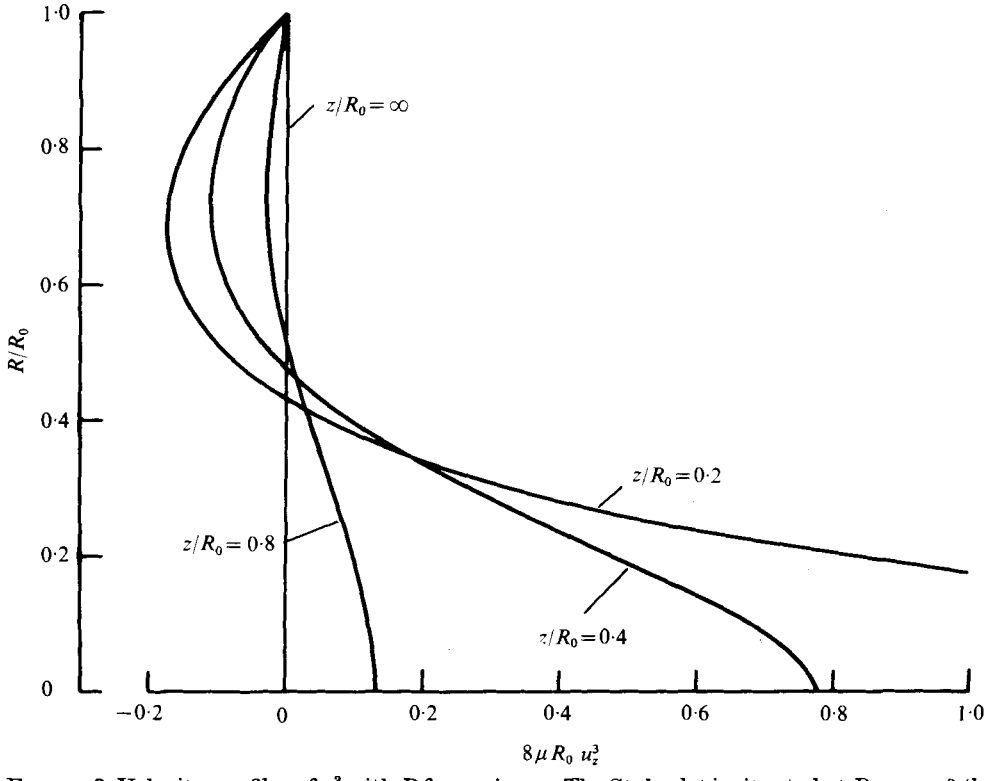

FIGURE 3. Velocity profiles of u_z^3 with R for various z. The Stokeslet is situated at $R = z = 0$ ($b = 0$), pointing in the z direction. This flow is axisymmetric.

7. Numerical results

Some numerical results will be exhibited in this section. The most interesting case is the case of a Stokeslet pointing downstream, in the z direction, and we shall show results for u_z^3 and P^3, for several cases. The case $b = 0$ (Stokeslet on the axis) is depicted in figures 3–6. Figure 3 shows velocity profiles u_z^3 as a function of R, for various z. As this flow is axisymmetric, and the total flux through a cross-section must be zero, Liron 1978), each of these curves must satisfy

$$\int_0^1 R u_z^3(R, z)\, dR = 0.$$

The exponential decay of the velocities, with z, is exhibited in figure 4, and the approach of P^3 to P_∞^3, with $z \to \infty$, is shown in figure 5. Only $z > 0$ is shown since $P^3(R, z)$ is an odd function of z. It is seen that near the Stokeslet the pressure overshoots the value P_∞^3 and then decays towards it, while further away, radially, the pressure increases monotonically to its limiting value. Both the velocity and the pressure are already very close to their limiting values at a distance of one radius up or downstream.

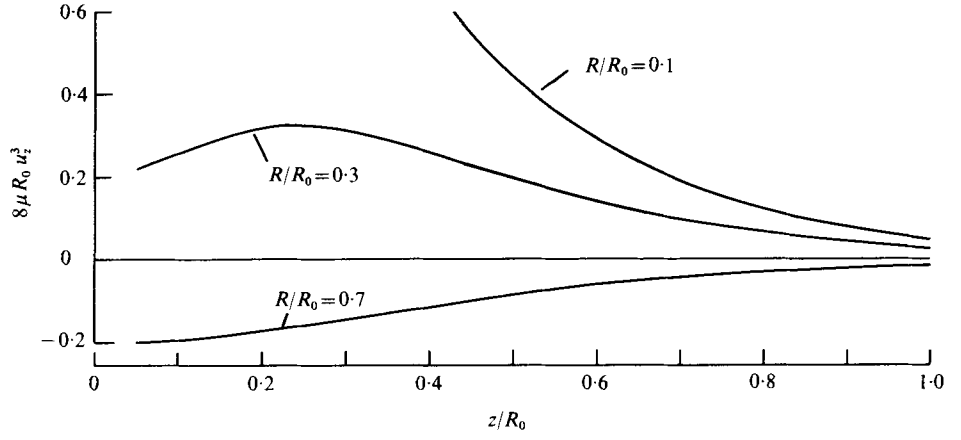

FIGURE 4. Variation of the velocity component u_z^3 along z depicting the exponential decay for various R. The Stokeslet is at $R = z = 0$ ($b = 0$), pointing in the z direction. This flow is axisymmetric.

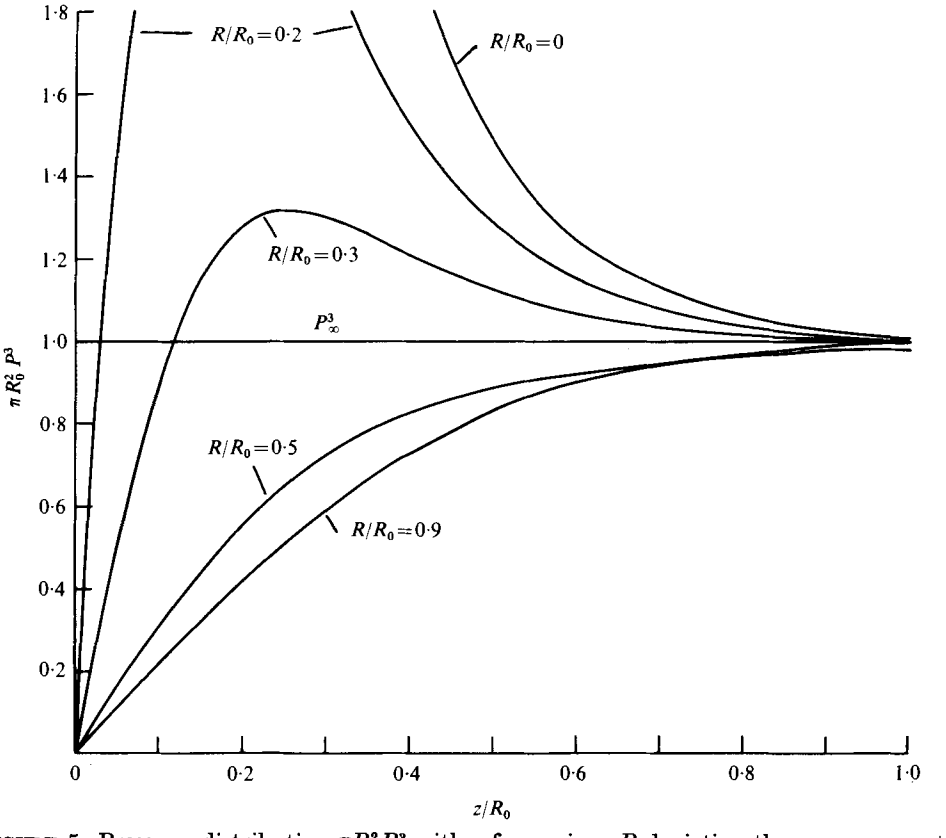

FIGURE 5. Pressure distribution $\pi R_0^2 P^3$ with z for various R depicting the convergence to P_∞^3. The Stokeslet is at $R = z = 0$ ($b = 0$), pointing in the z direction. This flow is axisymmetric.

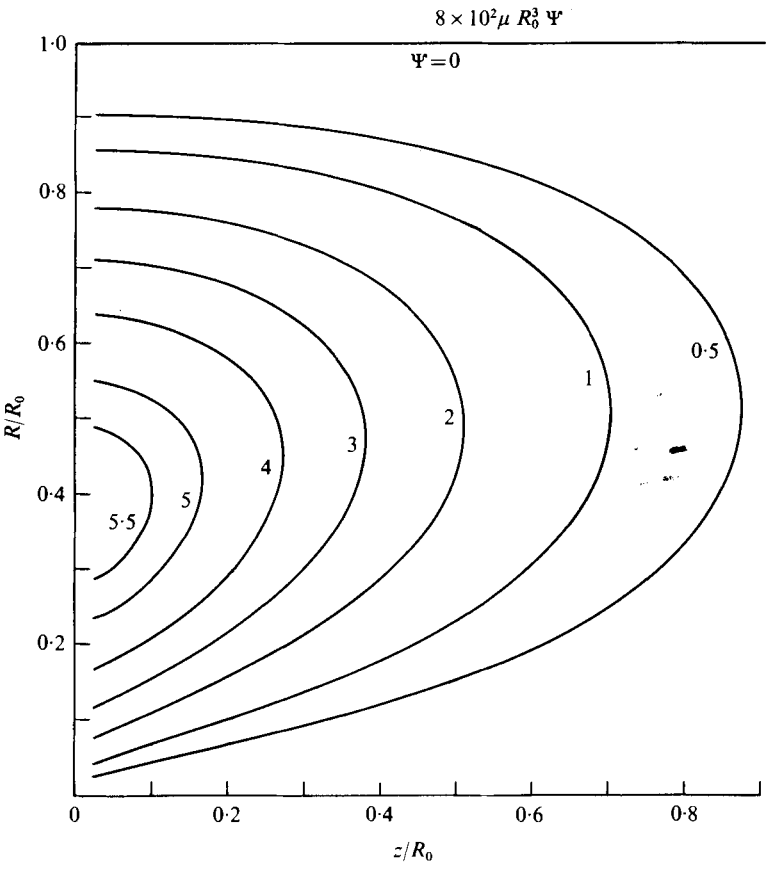

FIGURE 6. Streamlines in the pipe for a Stokeslet at $R = z = 0$ pointing in the z direction. This flow is axisymmetric.

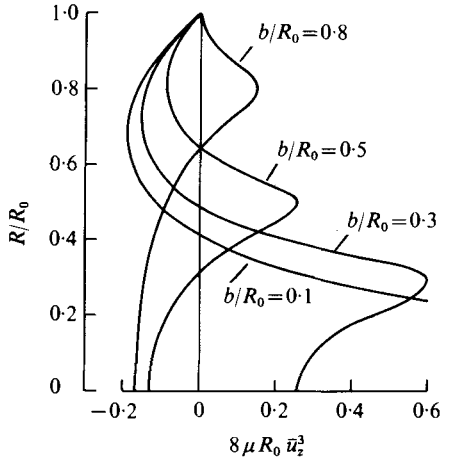

FIGURE 7. Velocity profiles $\bar{u}_z^3$ [see (7.3)] *vs.* R at $z = 0{\cdot}1R_0$, for a Stokeslet pointing in the z direction and situated at $R = bR_0$, $z = 0$, for various b.

For the case $b = 0$, and the Stokeslet in the z direction, one has axisymmetric flow, and one can define a stream function $\Psi = \Psi(z, R)$,

$$u_z^3 = \frac{1}{R}\frac{\partial \Psi}{\partial R}, \quad u_R^3 = -\frac{1}{R}\frac{\partial \Psi}{\partial z}. \tag{7.1}$$

This stream function can be found explicitly and is given by

$$\Psi = -2\pi \sum_{n=1}^{\infty} \exp(-b_n z)\,\mathrm{Im}\{\exp(ia_n z) \times [\psi^3(x_n, 0)\, R I_1(x_n R) + R^2 x_n I_1'(x_n R)\, \pi^3(x_n, 0)]/x_n D_0'(x_n)\}, \tag{7.2}$$

where $x_n = a_n + ib_n$ are the complex roots of $D_0(s)$ described in § 6, and ψ^3, π^3 are given in appendix B (with $b = 0$). Streamlines of $8\mu R_0^3 \Psi$ are given in figure 6, and are symmetric in z. We see that the Stokeslet creates a circulation (a rotating torus) the strength of which decays rapidly away from the Stokeslet.

The case $b \neq 0$ is more complicated since we have a true three-dimensional flow. For simplicity we shall exhibit results for the downstream velocity averaged over the angle Φ. Thus we define

$$\bar{u}_z^3(R, z) = \frac{1}{2\pi}\int_0^{2\pi} u_z^3(R, z, \Phi)\, d\Phi, \tag{7.3}$$

and in figure 7 we compare the average velocities $\bar{u}_z^3$ at $z = 0{\cdot}1R_0$ for several values of b. In all cases the Stokeslet at $R = b$, $z = 0$ is pointing in the z direction. We see that velocity is maximal opposite the singularity and compensates by becoming negative further away, to maintain zero flux. For $b = 0{\cdot}5R_0$ the velocity is negative (on the average) both closer to the wall and closer to the pipe axis. The maximum velocity diminishes the closer the Stokeslet is to the pipe wall. The same phenomena exist further downstream except for $b = 0{\cdot}5R_0$ the negative part closer to the wall becomes positive.

8. Discussion

We have given here the flow fields and pressures for Stokes flow due to a force singularity (Stokeslet) at arbitrary location and arbitrary orientation inside an infinite pipe. Two forms of the solution were given: one in a form of a Fourier–Bessel type expansion, and the other as a doubly infinite series. The second form is particularly amenable to computational purposes as it has been shown to be an exponentially decaying series.

All velocity components were shown to decay exponentially, away from the Stokeslet, up- or downstream. This was also true of the pressures for Stokeslets perpendicular to the axis. For a Stokeslet parallel to the axis the pressure field rises from a value of

$$-(1-(b/R_0)^2)/\pi R_0^2 \quad \text{at} \quad z = -\infty \quad \text{to} \quad +(1-(b/R_0)^2)/\pi R_0^2 \quad \text{at} \quad z = +\infty.$$

The approach to these values is also exponential with z. These results are the same as for a uniform distribution of equal strength Stokeslets on a line parallel to, and between, two flat plates, where z is the direction normal to the line, as shown by Liron (1978). These results are important in modelling cilia fluid transport in a pipe, by approximating this flow by a flow between two parallel plates, Liron (1978).

The flux due to a Stokeslet in a pipe is zero. This follows since the flux is equal at every cross-section, by incompressibility, and is bounded by the cross-sectional area,

times the maximum velocity over the cross-section, and the latter goes to zero as $z \to \infty$. The exponential decay of the velocities makes it possible to change the order of summation and integration when computing the flux due to an infinite sequence of Stokeslets situated along the pipe from $z = -\infty$ to $z = +\infty$ (force per unit length parallel to pipe axis, z) and therefore in this case we again get zero flux. Non-zero flux will then come only from adding a Poiseuille flow, as is discussed in the parallel-plates case by Liron (1978).

As in the case of flow between parallel plates, there will be a pressure rise per unit length associated with a uniform force per unit length, F, along z (and pointing downstream). This pressure rise is equal to $\Delta p = 2F(1-(b/R_0)^2)/\pi R_0^2$, and is equal to the pressure rise created by one Stokeslet of strength F, from $z = -\infty$, to $z = +\infty$.

For a single Stokeslet between, and parallel to, two plates, the flow field one gets is a circulation in planes parallel to the plates, which extends to infinity, see Liron & Mochon (1976*b*). For a Stokeslet in a pipe parallel to the axis we obtain a torus-shaped circulation. This difference is due to the fact that in a pipe there is no infinite lateral direction to the axis, unlike a single Stokeslet between parallel plates. The proper comparison should be between a single Stokeslet in a pipe and a uniform distribution of Stokeslets along a line between parallel plates, as mentioned above, and discussed by Liron (1978).

The exponential decay of velocities is also important in modelling cilia in a pipe because, in order to find the velocity field caused by an infinite array of cilia, we distribute Stokeslets along each cilium, and then sum over the entire infinite (in the z direction) array, see Blake (1972), Liron & Mochon (1976*a*), Liron (1978). The exponential decay with $|z|$ of velocity components due to each Stokeslet ensures us the possibility of such a summation.

This research was supported in part by the U.S. Army Research Office, Durham (grant DAAG-29-76-G-0315), while one of the authors (N. L.) was a Visiting Associate Professor with the Department of Mathematical Sciences, at Rensselaer Polytechnic Institute, summer 1976.

Appendix A

The functions f_j^i, t^i used in (3.6), (3.7) are as follows. For $R > b$,

$$f_1^1(\lambda,R,k,b) = K_k(\lambda R)\,[I_k(\lambda b) - \lambda b I_k'(\lambda b)] + \tfrac{1}{2}\lambda R[K_{k-1}(\lambda R)\,I_{k-1}'(\lambda b) + K_{k+1}(\lambda R)\,I_{k+1}'(\lambda b)],$$

$$f_2^1(\lambda,R,k,b) = \tfrac{1}{4}\lambda R[K_{k-1}(\lambda R)\,I_{k-2}(\lambda b) - K_{k+1}(\lambda R)\,I_{k+2}(\lambda b)] - \tfrac{1}{2}kK_k(\lambda R)\,I_k(\lambda b),$$

$$f_3^1(\lambda,R,k,b) = \tfrac{1}{2}\lambda R[K_{k-1}(\lambda R)\,I_{k-1}(\lambda b) + K_{k+1}(\lambda R)\,I_{k+1}(\lambda b)] - \lambda b K_k(\lambda R)\,I_k(\lambda b),$$

$$f_2^2(\lambda,R,k,b) = \tfrac{1}{2}I_k(\lambda b)\,[2K_k(\lambda R) - \lambda R K_k'(\lambda R)] - \tfrac{1}{4}\lambda R[K_{k+1}(\lambda R)\,I_{k+2}(\lambda b) + K_{k-1}(\lambda R)\,I_{k-2}(\lambda b)],$$

$$f_3^2(\lambda,R,k,b) = \tfrac{1}{2}\lambda R[K_{k-1}(\lambda R)\,I_{k-1}(\lambda b) - K_{k+1}(\lambda R)\,I_{k+1}(\lambda b)],$$

$$f_3^3(\lambda,R,k,b) = I_k(\lambda b)\,[2K_k(\lambda R) + \lambda R K_k'(\lambda R)] + \lambda b I_k'(\lambda b)\,K_k(\lambda R),$$

$$t^1(\lambda,R,k,b) = \lambda K_k(\lambda R)\,I_k'(\lambda b),$$

$$t^2(\lambda,R,k,b) = \frac{k}{b}K_k(\lambda R)\,I_k(\lambda b),$$

$$t^3(\lambda,R,k,b) = \lambda K_k(\lambda R)\,I_k(\lambda b),$$

where a prime denotes differentiation with respect to the argument.

For $R < b$ interchange the functions I and K throughout, and for f_2^2 change also the sign of the second square brackets from a minus to a plus. For f_2^1 change the sign of the square brackets from plus to minus.

Appendix B

The detailed expressions for all velocities and pressures, using the procedure described in § 5, for $z > 0$, are as follows. Let

$$A(F(s)) = -2\pi \sum_{n=1}^{\infty} \exp(-b_n z)\,\mathrm{Im}\,[\exp(ia_n z)\,F(x_n)] - \pi \sum_{n=1}^{\infty} \exp(-c_n z)\,\mathrm{Im}\,[F(y_n)], \tag{B 1}$$

and

$$B(F) = 2\pi \sum_{n=1}^{\infty} \exp(-b_n z)\,\mathrm{Re}\,[\exp(ia_n z)\,F(x_n)] + \pi \sum_{n=1}^{\infty} \exp(-c_n z)\,\mathrm{Re}\,[F(y_n)], \tag{B 2}$$

where Re stands for the real part, Im for the imaginary part, and $x_n = a_n + ib_n$, $y_n = ic_n$ are given in § 6, and are functions of k.

We then have

$$\left.\begin{aligned}
u_R^j &= \sum_{k=-\infty}^{\infty} \{[A(F_R^1(s,k))\,\delta_{j1} + B(F_R^3(s,k))\,\delta_{j3}]\cos k\Phi + A(F_R^2(s,k))\,\delta_{j2}\sin k\Phi\},\\
u_\Phi^j &= \sum_{k=-\infty}^{\infty} \{[A(F_\Phi^1(s,k))\,\delta_{j1} + B(F_\Phi^3(s,k))\,\delta_{j3}]\sin k\Phi + A(F_\Phi^2(s,k))\,\delta_{j2}\cos k\Phi\},\\
u_z^j &= \sum_{k=-\infty}^{\infty} \{[B(F_z^1(s,k))\,\delta_{j1} + A(F_z^3(s,k))\,\delta_{j3}]\cos k\Phi + B(F_z^2(s,k))\,\delta_{j2}\sin k\Phi\},\\
P^j &= 2\sum_{k=-\infty}^{\infty} \{[A(l^1(s,k))\,\delta_{j1} + B(l^3(s,k))\,\delta_{j3}]\cos k\Phi + A(l^2(s,k))\,\delta_{j2}\sin k\Phi\}\\
&\quad + \pi^{-1}(1-b^2)\,\delta_{j3}, \quad j = 1,2,3.
\end{aligned}\right\} \tag{B 3}$$

To give the functions F^j, l^j in (B 3), let

$$\left.\begin{aligned}
C_1(a(s),b(s),c(s),k) &= [a(s)\,I_k'(sR) + b(s)\,kI_k(sR)/sR + c(s)\,sRI_k''(sR)]/D_k'(s),\\
C_2(a(s),b(s),c(s),k) &= [a(s)\,kI_k(sR)/sR + b(s)\,I_k'(sR) + kc(s)\,(I_k(sR)/sR - I_k'(sR))]/D_k'(s),\\
C_3(a(s),c(s),k) &= [a(s)\,I_k(sR) + [sRI_k'(sR) + I_k(sR)]\,c(s)]/D_k'(s),\\
C_4(c(s),k) &= sc(s)\,I_k(sR)/D_k'(s),
\end{aligned}\right\} \tag{B 4}$$

and

$$\left.\begin{aligned}
d_1(\alpha(s),\beta(s),\gamma(s),k) &= -s[I_{k-1}(s)\,I_{k+1}(s)]'\,\alpha(s) - (sI_k(s))'\,[\beta(s)\,I_{k-1}(s) + \gamma(s)\,I_{k+1}(s)],\\
d_2(\alpha(s),\beta(s),\gamma(s),k) &= s(I_{k-1}(s)\,I_{k+1}'(s) - I_{k-1}'(s)\,I_{k+1}(s))\,\alpha(s)\\
&\quad + [(sI_k(s))'\,I_{k-1}(s) - sI_k(s)\,I_{k-1}'(s)]\,\beta(s)\\
&\quad + [(sI_k(s)\,I_{k+1}'(s) - (sI_k(s))'\,I_{k+1}(s)]\,\gamma(s),\\
d_3(\alpha(s),\beta(s),\gamma(s),k) &= 2\alpha(s)\,I_{k-1}(s)\,I_{k+1}(s) + I_k(s)\,[\beta(s)\,I_{k-1}(s) + \gamma(s)\,I_{k+1}(s)],
\end{aligned}\right\} \tag{B 5}$$

then the functions in (B 3) can be expressed as follows:

$$\left.\begin{aligned} F^j_R(s,k) &= (\delta_{j1}+\delta_{j3})\,C_1(\psi^j(s,k),\omega^j(s,k),\pi^j(s,k),k)\\ &\quad+\delta_{j2}C_1(\psi^2(s,k),-\omega^2(s,k),\pi^2(s,k),k),\\ F^j_\Phi(s,k) &= (\delta_{j1}+\delta_{j3})\,C_2(-\psi^j(s,k),-\omega^j(s,k),\pi^j(s,k),k)\\ &\quad+\delta_{j2}C_2(\psi^2(s,k),-\omega^2(s,k),-\pi^2(s,k),k),\\ F^j_z(s,k) &= (\delta_{j3}-\delta_{j1}-\delta_{j2})\,C_3(\psi^j(s,k),\pi^j(s,k),k),\\ l^j(s,k) &= C_4(\pi^j(s,k),k),\quad j=1,2,3, \end{aligned}\right\} \tag{B 6}$$

where

$$\left.\begin{aligned} \psi^j(s,k) &= d_1(L^j(s,k),H^j(s,k),G^j(s,k),k),\\ \omega^j(s,k) &= d_2(L^j(s,k),H^j(s,k),G^j(s,k),k)\,(\delta_{j1}-\delta_{j2}+\delta_{j3}),\\ \pi^j(s,k) &= d_3(L^j(s,k),H^j(s,k),G^j(s,k),k),\quad j=1,2,3. \end{aligned}\right\} \tag{B 7}$$

The functions L^j, H^j, G^j are

$$\left.\begin{aligned} 4\pi^2L^1(s,k) &= -\tfrac{1}{2}s[K_{k-1}(s)\,I_{k-1}(sb)+K_{k+1}(s)\,I_{k+1}(sb)]+sbK_k(s)\,I_k(sb),\\ 4\pi^2H^1(s,k) &= \tfrac{1}{2}sI_{k+1}(sb)\,K'_{k+1}(s)-\tfrac{1}{2}sK_k(s)\,I_{k-1}(sb)\\ &\quad+\tfrac{1}{2}K_{k+1}(s)\,[sb(I_k(sb)+I'_{k+1}(sb))-2I_{k+1}(sb)],\\ 4\pi^2G^1(s,k) &= \tfrac{1}{2}sI_{k-1}(sb)\,K'_{k-1}(s)-\tfrac{1}{2}sK_k(s)\,I_{k+1}(sb)\\ &\quad+\tfrac{1}{2}K_{k-1}(s)\,[sb(I_k(sb)+I'_{k-1}(sb))-2I_{k-1}(sb)], \end{aligned}\right\} \tag{B 8}$$

$$\left.\begin{aligned} 4\pi^2L^2(s,k) &= -\tfrac{1}{2}s[K_{k-1}(s)\,I_{k-1}(sb)-K_{k+1}(s)\,I_{k+1}(sb)],\\ 4\pi^2H^2(s,k) &= (k+2)\,K_{k+1}(s)\,I_{k+1}(sb)-\frac{k}{b}K_k(s)\,I_k(sb),\\ 4\pi^2G^2(s,k) &= (k-2)\,K_{k-1}(s)\,I_{k-1}(sb)-\frac{k}{b}K_k(s)\,I_k(sb), \end{aligned}\right\} \tag{B 9}$$

and

$$\left.\begin{aligned} 4\pi^2L^3(s,k) &= I_k(sb)\,[2K_k(s)+sK'_k(s)]+sbK_k(s)\,I'_k(sb),\\ 4\pi^2H^3(s,k) &= s[bK_{k+1}(s)\,I_{k+1}(sb)-K_k(s)\,I_k(sb)],\\ 4\pi^2G^3(s,k) &= s[bK_{k-1}(s)\,I_{k-1}(sb)-K_k(s)\,I_k(sb)]. \end{aligned}\right\} \tag{B 10}$$

In all expressions above, a prime denotes differentiation with respect to the argument. $D_k(s)$ appearing in (B 4) is given in (5.1).

In (B 3) there is no contribution from $k=0$ for these expressions which have $\sin k\Phi$ under the sum. For those sums with $\cos k\Phi$ there is a contribution from $k=0$. It turns out that in these cases, for $k=0$, both numerator and denominator in (5.2) have a common factor $I_1(s)$. $I_1(s)$ contributes the roots y_n on the imaginary axis in this case and it follows that for $k=0$ one should omit the second sum in (B 1), (B 2). The one exception is u^2_Φ, for which $I_1(s)$ does not appear in the numerator, but rather that part contributing the complex roots x_n is a common factor. In this case then, one should omit the first sum in (B 1), for $k=0$.

REFERENCES

ABRAMOWITZ, M. A. & STEGUN, I. A. 1965 *Handbook of Mathematical Functions.* Dover.

BLAKE, J. R. 1971 A note on the image system for a Stokeslet in a no-slip boundary. *Proc. Camb. Phil. Soc.* **70**, 303–310.

BLAKE, J. R. 1972 A model for the micro-structure in ciliated organisms. *J. Fluid Mech.* **55**, 1–23.

BLAKE, J. R. & SLEIGH, M. A. 1974 Mechanics of ciliary locomotion. *Biol. Rev.* **49**, 85–125.

HAPPEL, J. & BRENNER, H. 1973 *Low Reynolds Number Hydrodynamics, with Special Applications to Particulate Matter*, 2nd rev. ed. Leiden: Noordhoff.

LARDNER, T. J. & SHACK, W. J. 1972 Cilia transport. *Bull. Math. Biophys.* **34**, 325–335.

LIRON, N. 1978 Fluid transport by cilia between parallel plates. *J. Fluid Mech.* **86**, 705–726.

LIRON, N. & MOCHON, S. 1976*a* The discrete-cilia approach to propulsion of ciliated microorganisms. *J. Fluid Mech.* **75**, 593–607.

LIRON, N. & MOCHON, S. 1976*b* Stokes flow for a Stokeslet between two parallel flat plates. *J. Engng Math.* **10**, 287–303.

LORENTZ, H. A. 1896 *Zittingsverlag. Akad. v. Wet.* **5**, 168–182.